buildings

MDPI

Article

Crack Self-Healing of Cement Mortar Containing Ureolytic Bacteria Immobilized in Artificial Functional Carrier under Different Exposure Environments

Mian Luo [1,2,*], Ye Liu [1,2], Xu Li [1,2] and Junjie Dai [1,2]

[1] College of Civil Science and Engineering, Yangzhou University, Yangzhou 225127, China
[2] Research Institute of Green Building Materials, Yangzhou University, Yangzhou 225127, China
* Correspondence: luomian@yzu.edu.cn

Abstract: The ureolytic bacteria and nutrients were immobilized in the artificial functional carrier (AFC) and the self-healing cement mortar, based on the AFC-encapsulated bacteria, was prepared for this paper. The crack self-healing effect of mortars with and without bacteria under different exposure environments (standard curing, dry–wet cycle curing, and water curing) was investigated by the visual observation of surface and internal cracks, water permeability tests, and mechanical performance recovery. In addition, the internal healing products of the cracks were observed using the metallographic microscope. The results show that the mortar specimens containing ureolytic bacteria immobilized in artificial functional carrier have a higher crack area repair ratio, and better water tightness regain and recovery ratio of flexural strength compared with the control mortars under the same exposure environment. The self-healing effect of mortar cracks with and without bacteria is obviously affected by the exposure environments. The self-healing effect of the cracks are the best when the mortar specimens are cured in water, followed by dry–wet cycle curing, and the self-healing effect of the cracks is the worst in standard curing, indicating that the presence of water is necessary for crack self-healing. The mortar specimens with bacteria generate more repair products in the surface and interior of the cracks to greatly improve the self-repair ability of the specimens, which promotes the recovery of water tightness and mechanical performance.

Keywords: cement mortar; crack; bacteria; self-healing; artificial carrier; exposure environments

Citation: Luo, M.; Liu, Y.; Li, X.; Dai, J. Crack Self-Healing of Cement Mortar Containing Ureolytic Bacteria Immobilized in Artificial Functional Carrier under Different Exposure Environments. *Buildings* **2022**, *12*, 1348. https://doi.org/10.3390/buildings12091348

Academic Editor: Shazim Memon

Received: 15 July 2022
Accepted: 27 August 2022
Published: 1 September 2022

1. Introduction

Concrete is widely used in the field of construction engineering because it is an easy material to obtain, the low price, and excellent compressive strength. However, concrete is a brittle material with low tensile strength, and it is easy for cracks to form, which causes water and harmful media to accelerate the erosion of the concrete interior, resulting in a greatly reduced durability [1–4]. Therefore, the need to develop efficient, active crack-repairing technologies is urgent and important [5–7]. In recent years, microbially induced calcium carbonate precipitation (MICP) technology was proposed for crack self-healing of cementitious materials [8–13]. For this application, the specific bacteria were added to the concrete mixture when mixing and, once the concrete cracks, the embedded bacteria induce the formation of calcium carbonate to repair the crack. To ensure the survival of the bacteria in the cement matrix, protective techniques are often adopted [14,15]. In the current research results, calcium sulphoaluminate cement [16,17], ceramsite [18], expanded shale [19], limestone powder [20], diatomite [21], hydrogel [22,23], microcapsule [24,25], expanded perlite [26], recycled aggregate [27], and sodium alginate [28] were used as carriers to provide a suitable environment for the germination and growth of bacteria. After the bacteria were protected by the carrier, the crack repair effect significantly improved. However, the compatibility of the carrier materials with the concrete needs to be further studied and improved. The ideal carrier materials for bacteria should not have a great negative impact on the working performance, mechanical performance, or durability of the concrete, and the preparation of the carrier and the bacteria immobilization process should also be economic and environmentally friendly. In addition, the existing research results [12] show that calcium carbonate induced by bacteria can seal the crack well, but the internal repair effect of the crack is not ideal, due to decreased bacterial activity in the depth of the crack. Therefore, the development of multifunctional bacterial carriers, which can use their own components to promote the repair of internal cracks while protecting bacteria, may be an alternative solution.

Moreover, the environmental conditions of concrete structures vary greatly due to the difference in latitude and longitude, such as dry environments, underwater environments, and dry–wet cycle environments, etc. Therefore, the self-repairing environment is obviously different, and need to be considered when evaluating the self-healing efficiency of concrete cracks. Wang et al. [24] found that the crack-healing effect is poor for bacteria-based self-healing concrete placed in environments with relative humidity of 60%, 95%, and above 95%; however, large amounts of calcium carbonate precipitations were observed in the cracks of specimens for healing in water, indicating that water is the important factor in the repair process of concrete cracks. Snoeck et al. [29], Luo et al. [30], and Flores et al. [31] also testified that water is an important factor in the self-repairing of concrete cracks. In addition to placing concrete specimens in water for repair, the researchers also studied the self-healing of concrete specimens in nutrient solutions. Farzaneh et al. [32] found that cracked concrete repairs better in the urea–calcium chloride mixture solution than in water. Wang et al. [33] compared the repair effects of self-healing concrete in water and in nutrient solutions containing calcium nitrate–urea, and found that the latter produced more calcium carbonate, and the cracks were better repaired.

The main objective of this research is to develop a new artificial functional carrier (AFC) based on our previous work [34], and investigate the crack self-healing effect of cement mortar containing ureolytic bacteria immobilized in the AFC under different exposure environments (standard curing, dry–wet cycle curing, and water curing). For the evaluation of self-healing efficiency, the visual observation of surface and internal cracks, water permeability tests, and mechanical performance recovery were conducted. In addition, the internal healing products of the cracks were observed and analyzed using a metallographic microscope.

2. Materials and Methods

2.1. Bacterial Strain

The ureolytic bacteria strain used in the study was sporosarcina pasteurii, which was purchased from the China General Microbiological Culture Collection Center (CGMCC). After the bacteria were activated, they were inoculated into a sterile liquid medium and grown in a thermostatic oscillator (30 °C, 180 rpm) for 36 h. The composition of liquid culture media (pH is about 8.0) was 20 g/L yeast extract and 20 g/L urea. The culture medium was then centrifuged at 8000 rpm for 5 min to obtain highly concentrated bacterial cells.

2.2. Bacteria and Nutrient Immobilization Process

The highly concentrated bacterial cells were resuspended in deionized water, and the bacterial suspension was sprayed evenly on calcium carbonate powder. After drying in an oven at 40 °C, the bacteria-carrying calcium carbonate powder was mixed well with granulated blast furnace slag, sodium carbonate, and yeast extract. The mixed materials were made into pellets in a disc granulator. In addition, the pellets were coated with a layer of epoxy resin solution evenly and placed on the tray. Then, a small amount of sulphoaluminate cement was sprinkled on the surface of the pellets to prevent the particles from sticking together. After curing for 24 h, the pellets coated with epoxy resin were put into the disc granulator again, to wrap them with a sulphoaluminate cement shell. After that, the pellets were taken out and placed in a curing room at 20 °C and 95% humidity for 3 days. The artificial-functional-carrier-encapsulated bacteria with a particle size of

1.18–4.75 mm were obtained (Figure 1) and used in this study. The density of the artificial functional carrier encapsulated bacteria is 2.15 g/cm^3.

Figure 1. The artificial-functional-carrier-encapsulated bacteria.

2.3. *Preparation of Mortar Specimens*

According to the mixing proportions of cement mortars in Table 1, the cylindrical and prismatic cement mortar specimens were prepared. The dimensions and purposes of each specimen are shown in Table 2. The water to binder ratio of mortar is 0.5 and the binder to sand ratio is 1:3 for the control mortars. To prepare the mortars with bacteria, the amount of artificial-functional-carrier (AFC)-encapsulated bacteria is 10% of the volume of mortar mixture, and the sand is replaced by the same volume of AFC. The content of both urea and calcium lactate is 1% of cement mass. At the same time, the polypropylene fibers with a diameter of 31 μm and a length of 12 mm (0.1% by volume) were added to maintain the integrity of the sample after cracking. All specimens were demolded after 24 h of casting, and maintained in the standard curing room (20 ± 2 °C, RH > 95%) until 28 days of age.

Table 1. Mixing proportions of cement mortars.

Mix.	Cement (g)	Sand (g)	Water (g)	AFC (g)	Urea(g)	Calcium Lactate (g)	PP Fiber (g)
Control	450	1350	225	/	/	/	0.7
With bacteria	450	1116	225	190	4.5	4.5	0.7

Table 2. Dimensions and purposes of each specimen.

Dimensions of Mortar Specimens	Purposes
160 mm × 40 mm × 40 mm	The recovery effect of mechanical performance evaluation.
Φ100 mm × 25 mm	Repair effect of crack surface and the regain of water tightness.
Φ50 mm × 25 mm	The observation of crack internal healing products.

2.4. *Methods of Making Cracks*

Crack creation of cylindrical mortar specimens followed the method described in [34]. After curing for 28 d, a crack with a width of about 0.4 mm was produced in the cylindrical specimens by splitting tensile strength test. For the prismatic specimens, cracks were created by means of three-point bending test. The loading speed was set to 20 N/s, and the loading was stopped immediately after the specimens were pressurized until cracks appeared. Subsequently, the cracked specimens were hold by rubber bands and crack width was controlled by inserting the pins. In order to accurately measure the flexural strength of mortar specimens after repairing, the crack width was not too large. After many attempts, the crack width was controlled at about 0.1 mm.

2.5. Exposure Environments

All pre-cracked specimens were placed in three different exposure environments (standard curing, dry–wet cycle curing, and water curing) for healing. The standard curing involved putting the pre-cracked mortar specimens in the standard curing room (20 ± 2 °C, RH > 95%) for healing. For the dry–wet cycle curing, the pre-cracked specimens were submerged in water for 12 h of healing, and then taken out to air-dry for 12 h of healing in each cycle. The water curing involved putting the pre-cracked specimens into water for healing.

2.6. Evaluation Methods of Self-Repairing Performance

2.6.1. Repair Effect of Crack Surface

The digital photos of all marks along the cracks on the specimens before and after repairing were taken and recorded by stereomicroscope. The Image-J software was used to process the digital photos to obtain the binary images of crack. For image binarization, an appropriate threshold was determined to distinguish crack zones and the cement mortar matrix, according to the gray histogram of the photo. In this study, the photos taken under different repair times of the same crack were binarized with the same threshold. After image binarization, the crack zone on the photo turned black and the cement mortar matrix turned white. Due to the existence of pores, stains, and other defects, some black spots also appeared in the cement mortar matrix area and were removed manually. The number of pixels in the crack zone (black area) before and after repairing was counted by the Image-J software and used as the initial crack area (A_0) and the crack area after repairing (A_t). The crack area repair ratio R_A was calculated based on Equation (1) to evaluate the repair effect of crack surface.

$$R_A = \frac{A_0 - A_t}{A_0} \times 100\% \tag{1}$$

2.6.2. The Regain of Water Tightness

In order to evaluate the self-healing effect of crack indirectly, a device suitable for a water permeability test of self-healing cementitious materials was designed. Detailed information about the water permeability test device can be seen in our previously published paper [34]. The initial water permeability coefficient k_0 (cm/s) and the water permeability coefficient of specimens after healing for certain time k_t (cm/s) were obtained by the test device of water permeability. Then, the relative permeability coefficient (k_t/k_0) of different healing time was calculated to evaluate the regain of water tightness.

2.6.3. Recovery Effect of Mechanical Performance

The prismatic specimens were adopted to evaluate the recovery effect of mechanical performance after healing. After curing for 28 d in the standard curing room, the specimens were taken out and the initial flexural strength f_0 was obtained by three-point bending test on the testing machine of mechanics of materials. Then, the cracked specimens (crack width of about 0.1 mm) were exposed to different restoration environments for healing of 56 d. The three-point bending test was performed again on the healed specimens to obtain the flexural strength f_1. According to Equation (2), the recovery ratio of flexural strength R_f can be obtained.

$$R_f = \frac{f_1 - f_0}{f_0} \times 100 \tag{2}$$

2.7. Microscopic Investigation

After healing for 56 days, the mortar specimens were divided into two groups. One group was broken off along the original crack to directly observe the overall repair of the crack wall. The other group were sampled as described in [34], and the internal healing products of cracks were observed using a metallographic microscope.

3. Results and Discussion

3.1. Repair Effect of Crack Surface

Images of surface cracks in mortars with and without bacteria were taken after repairing for 0 d, 3 d, 14 d, 28 d, and 56 d under different exposure environments by stereo optical microscope (Figure 2). The images were binarized by the Image-J software, as shown in Figure 3. The crack area repair ratio of mortars was calculated based on the reduction in crack area after healing, as shown in Figure 4. It is found that cracks in mortar specimens with and without bacteria are barely repaired under the standard curing environment. Under the dry–wet cycle curing environment, the crack area repair ratio increases to 27.2% and 52.7% for the control mortar specimens and mortar specimens with bacteria, respectively. The crack area repair ratio of mortar specimens with bacteria under the water curing is 99.6%, much higher than the 43.7% of control mortar specimens. It is noticed the results are different than the results of Wang et al. [24]. Wang et al. [24] report that the wet–dry cycle condition is better than the water condition. The possible reasons are as follows: (1) the dry–wet cycle condition is different; (2) the bacteria carrier is different. According to the literature by Wang et al. [24], during one wet–dry cycle, the specimens were immersed in water for 16 h, and were then exposed to air for 8 h. In this study, the pre-cracked specimens were submerged in water for 12 h of healing and then taken out to air-dry for 12 h of healing in each cycle. A longer immersion time in water during one wet–dry cycle may result in sufficient water being available when the specimen is repaired in air. Meanwhile, when the specimens are exposed to the atmosphere, more oxygen becomes available for the bacteria than in the case of continuous immersion. Therefore, under the dry–wet cycle curing, the self-repairing effect of cracks may even exceed that of curing in water. In addition, the bacteria carrier used in this paper is different from that used by Wang et al. in their study. In this study, the bacteria and nutrients were immobilized in artificial functional carrier (AFC), and perhaps more water is needed to form repair products. Therefore, repairing the specimen in the air for a longer time during one wet–dry cycle may affect the final repair effect of the cracks. It is worth mentioning that both the research results by Wang et al. [24] and the research results of this paper show that the cracks have a good repair effect under the water condition and wet–dry cycle condition.

3.2. The Regain of Water Tightness

The improvement of the impermeability performance is an important indicator for self-healing cement-based materials. The change in the relative permeability coefficient of mortar specimens with and without bacteria after repairing for 0 d, 3 d, 14 d, 28 d, and 56 d under different exposure environments is shown in Figure 5. Compared with the control mortar specimens, it is found that the regain of water tightness of mortar specimens with bacteria is better under the water curing and dry–wet cycle curing environments. Under the standard curing environment, the regain of water tightness of mortar specimens with and without bacteria is poor. However, the regain of water tightness of mortar specimens is significantly enhanced under the water curing environment, indicating that the existence of water is necessary for crack-healing. For the control mortar specimens, crack self-healing mainly relies on the secondary hydration of dehydrated cement, precipitation of $CaCO_3$ due to the carbonation of calcium hydroxide, and swelling of hydration products. All these reaction processes need the participation of water. For the mortar specimens with bacteria encapsulated in the artificial functional carrier, in addition to the above reaction processes, the dissolution of substances and bacterial-induced calcium carbonate deposition also need water.

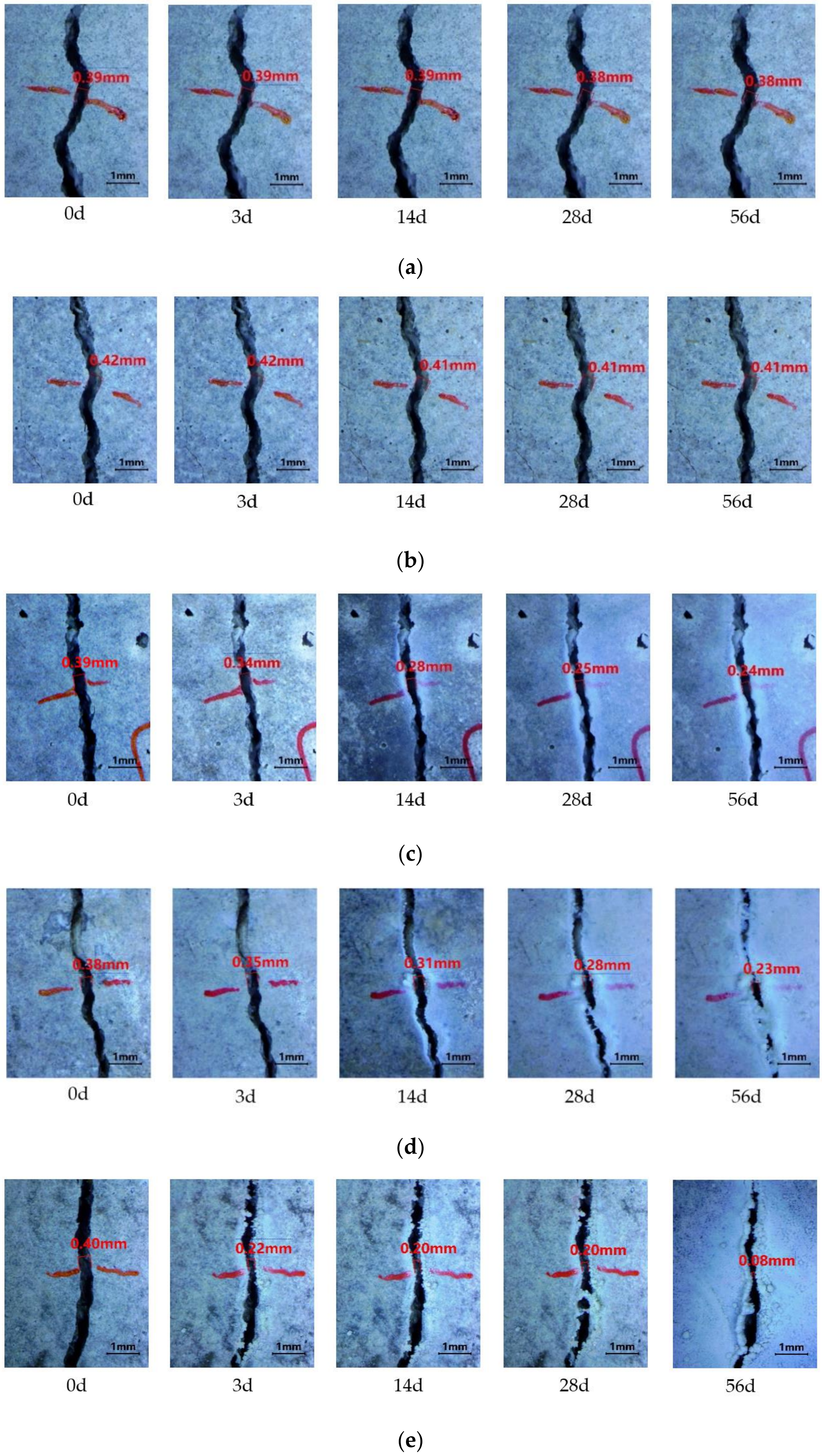

Figure 2. *Cont.*

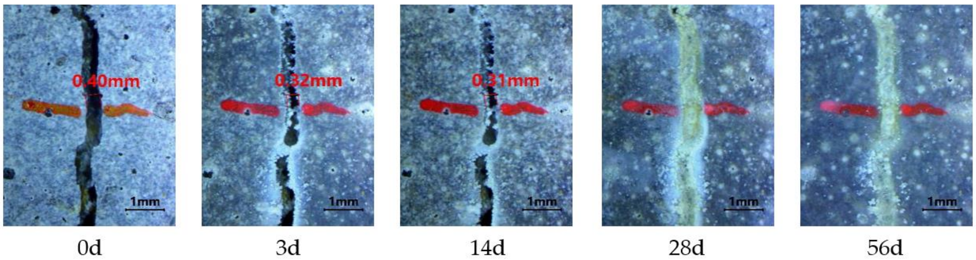

(**f**)

Figure 2. Self-healing images of surface crack in mortars under different exposure environments. (**a**) The control mortar specimens under the standard curing. (**b**) Mortar specimens with bacteria under the standard curing. (**c**) The control mortar specimens under the dry–wet cycle curing. (**d**) Mortar specimens with bacteria under the dry–wet cycle curing. (**e**) The control mortar specimens under the water curing. (**f**) Mortar specimens with bacteria under the water curing.

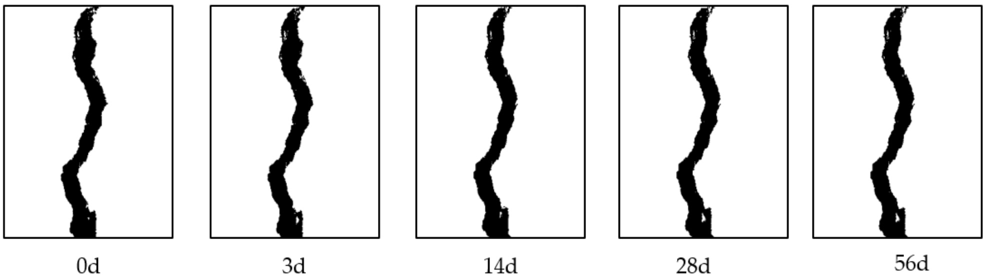

(**a**)

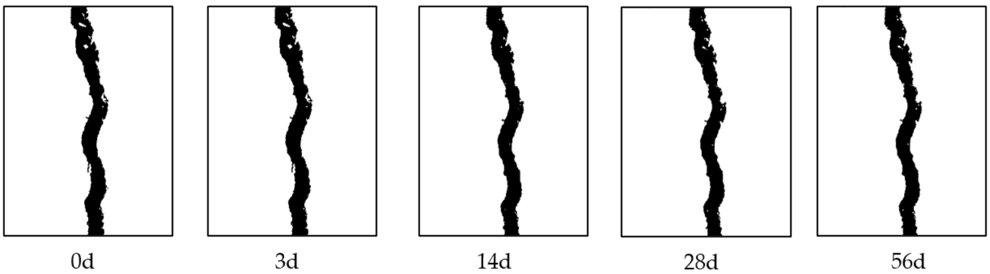

(**b**)

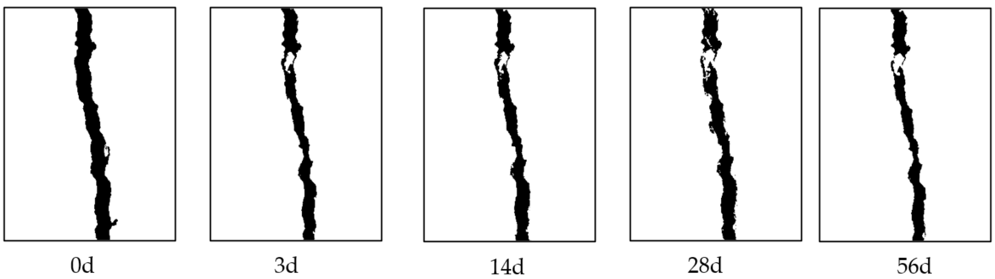

(**c**)

Figure 3. *Cont*.

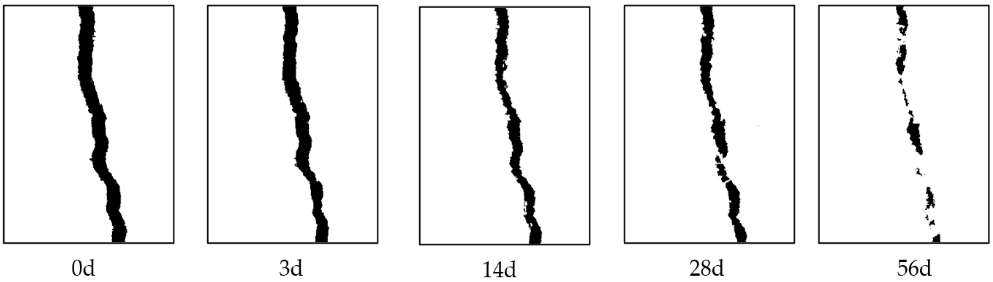

(**d**)

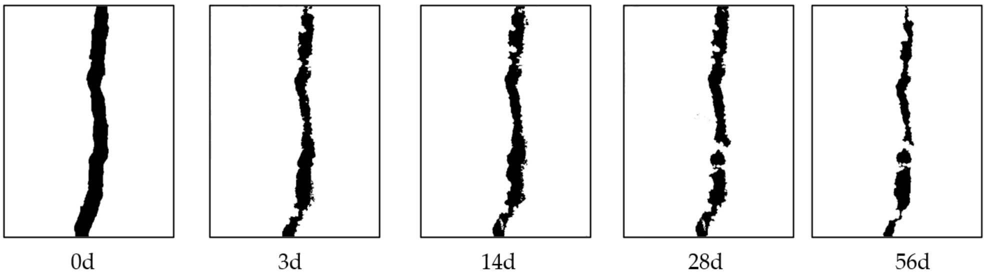

(**e**)

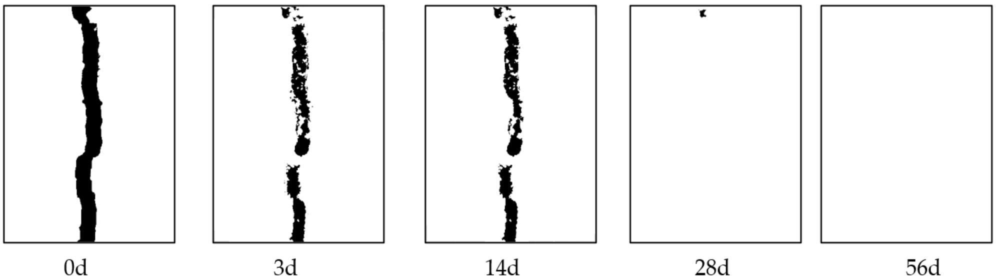

(**f**)

Figure 3. Binarized self-healing images of surface cracks in mortars under different exposure environments. (**a**) The control mortar specimens under the standard curing. (**b**) Mortar specimens with bacteria under the standard curing. (**c**) The control mortar specimens under the dry–wet cycle curing. (**d**) Mortar specimens with bacteria under the dry–wet cycle curing. (**e**) The control mortar specimens under the water curing. (**f**) Mortar specimens with bacteria under the water curing.

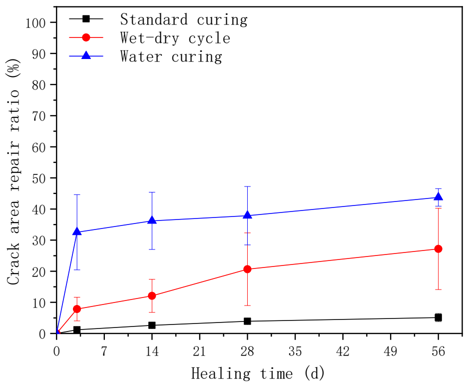

(**a**)

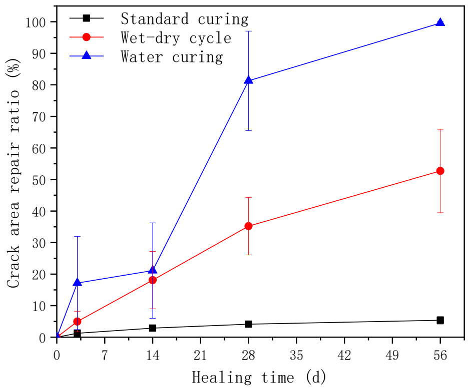

(**b**)

Figure 4. Crack area repair ratio of mortars under different exposure environments: (**a**) control; (**b**) with bacteria. Three specimens were tested for each exposure environment.

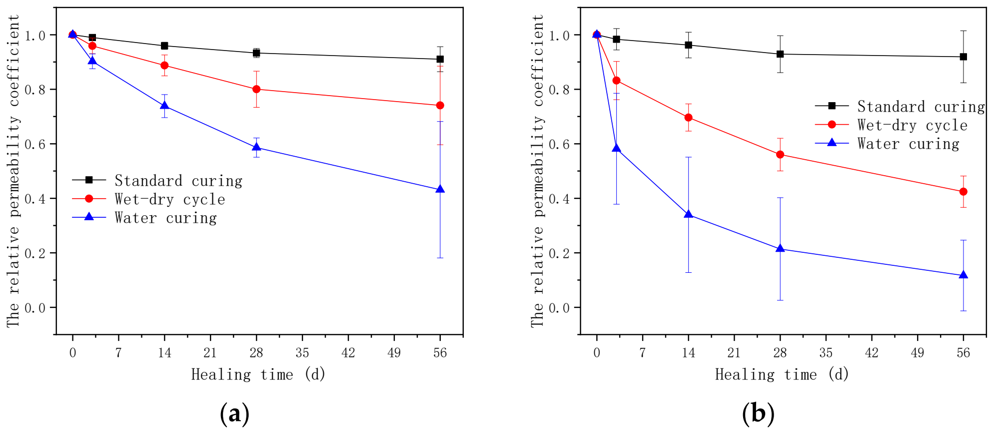

Figure 5. The relative permeability coefficient of mortar specimens under different exposure environments: (**a**) control; (**b**) with bacteria. Three specimens were tested for each exposure environment.

3.3. Recovery Effect of Mechanical Performance

The flexural strength recovery ratio of mortar specimens (crack width of 0.1 mm) after 56 days of repair under different exposure environments is shown in Figure 6. It can be seen that the mechanical performance recovery effect of mortar specimens is the best under the water curing environment, and then under the dry–wet cycle curing environment, while it is the worst under the standard curing environment. The mechanical performance recovery effect of mortar specimens with bacteria is higher than the control group under different exposure environments. The flexural strength recovery ratio of the control group under the standard curing, dry–wet cycle curing, and water curing environment is 8.6%, 10.4%, and 11.9%, respectively, while those of the mortar specimens with bacteria are 8.8%, 14.8%, and 20.3%, respectively. This is probably due to more repair products being generated in mortar specimens with bacteria.

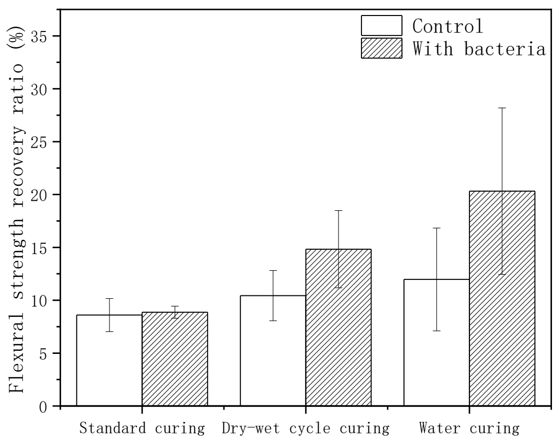

Figure 6. Flexural strength recovery ratio of mortar specimens under different exposure environments. Three specimens were tested for each exposure environment.

3.4. Microscopic Investigation

After healing for 56 d under different exposure environments, the mortar specimens were broken off along the original cracks, and the healing products on the crack walls were observed, as shown in Figure 7. It can be seen that the obvious white healing products are formed on the crack walls of mortar specimens under the dry–wet cycle curing and water curing environments' however, few white healing products are observed on the crack walls of mortar specimens under the standard curing environment, still showing the original color of cement matrix. The white healing products in control mortar specimens are limited to the opening around the crack, and fail to reach the crack inside under the dry–wet cycle curing and water curing environments; however, more healing products are found on the crack walls of mortar specimens with bacteria, and the healing products extend into the crack interior, indicating that the mortar specimens with bacteria have a better repair effect inside the crack. The white healing product is mainly calcium carbonate precipitation, in accordance with the previous study.

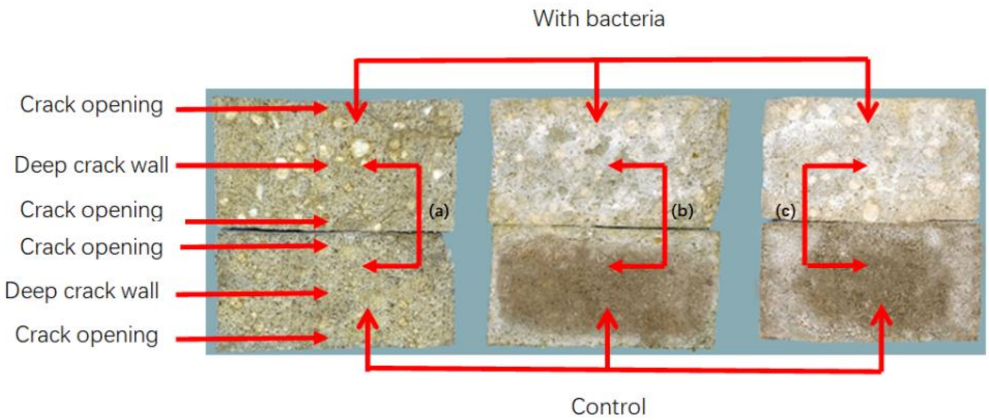

Figure 7. Healing products in crack wall of mortar specimens after healing for 56 d under different exposure environments: (**a**) standard curing; (**b**) dry–wet cycle; (**c**) water curing.

Meanwhile, in order to observe the healing effect of internal cracks more intuitively, after healing for 56 d, the mortar specimens were cured by resin impregnation and cut into small pieces to observe the internal healing products using the metallographic microscope. Figure 8 shows the healing products formed in the shallow cracks of mortar specimens under different exposure environments. It can be seen from Figure 8 that there are almost no healing products at the crack mouth of mortar specimens with and without bacteria under the standard curing environment. A thin layer of crystals on both sides of the cracks of control mortar specimens are formed, and extend to the crack mouth under the dry–wet cycle curing environment, but both sides of the cracks are not connected, while the crystals on both sides of the crack on mortar specimens with bacteria are thicker and completely block the crack mouth. More crystals are generated at the crack mouth of mortar specimens with and without bacteria under the water curing environment, which blocks the cracks well. This phenomenon is consistent with the previous surface repair effect of the cracks.

Figure 9 shows the healing products formed in deep cracks of the mortar specimens under different exposure environments. It is clear that almost no repair products are found within the cracks of all the control mortar specimens under different exposure environments. For the mortar specimens with bacteria, there is no generation of healing products within the crack under the standard curing environment. However, abundant healing products are found under dry–wet cycle curing and water curing environments. In summary, the mortar specimens with bacteria generate more repair products in the surface and interior of cracks to greatly improve the self-repair ability of the specimens, but the ability of repair products to form is closely related to the exposure environments.

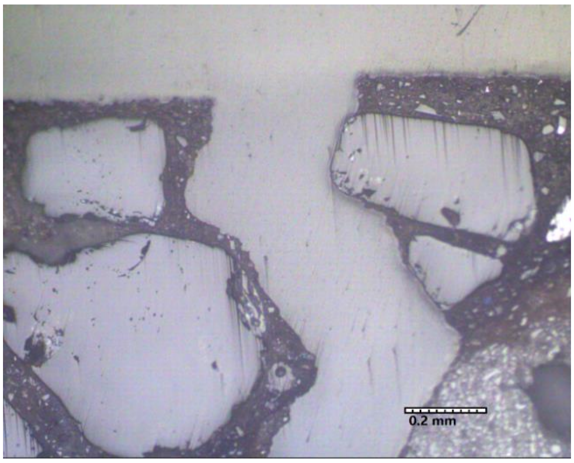

Standard curing

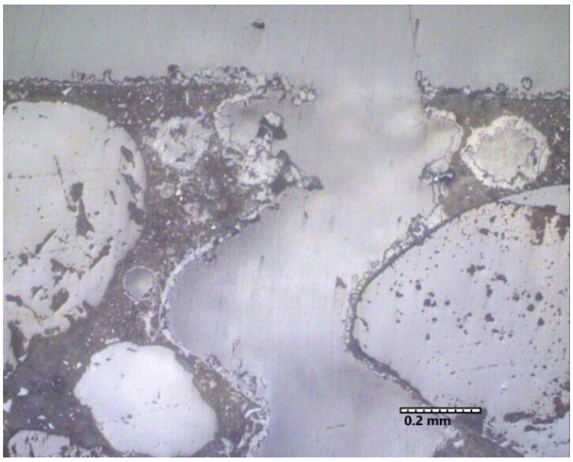

Dry-wet cycle curing

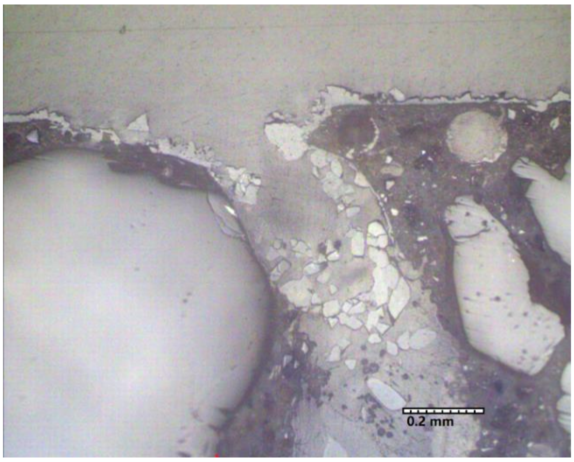

Water curing

(**a**)

Figure 8. *Cont*.

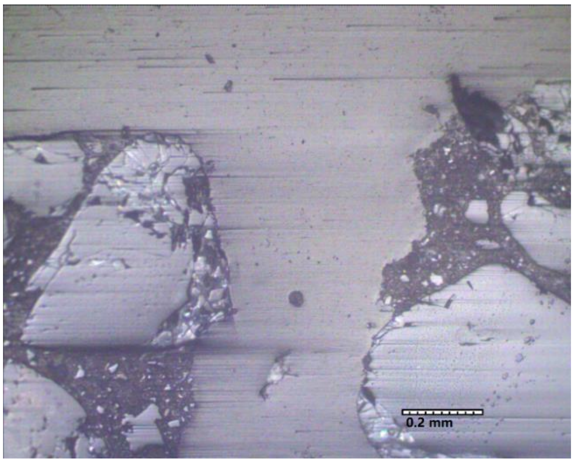

Standard curing

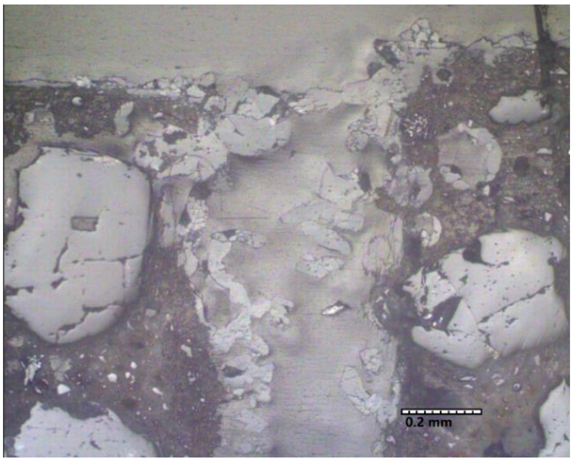

Dry-wet cycle curing

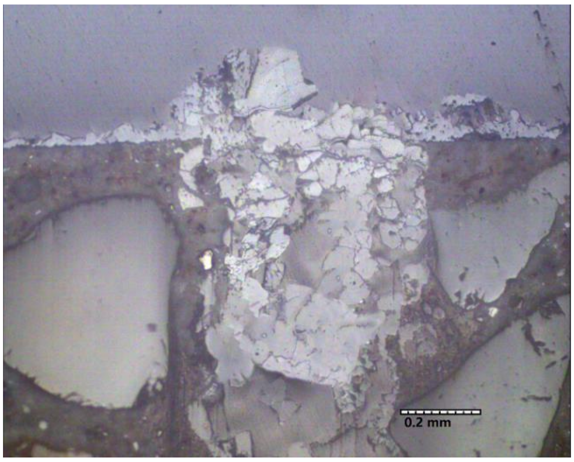

Water curing

(**b**)

Figure 8. Healing products in shallow cracks under different exposure environments: (**a**) control; (**b**) with bacteria.

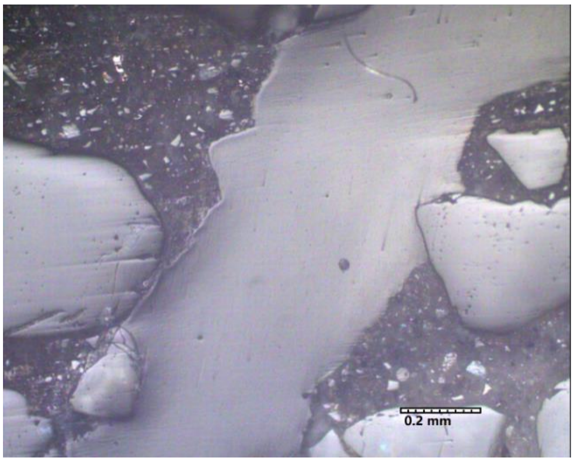

Standard curing

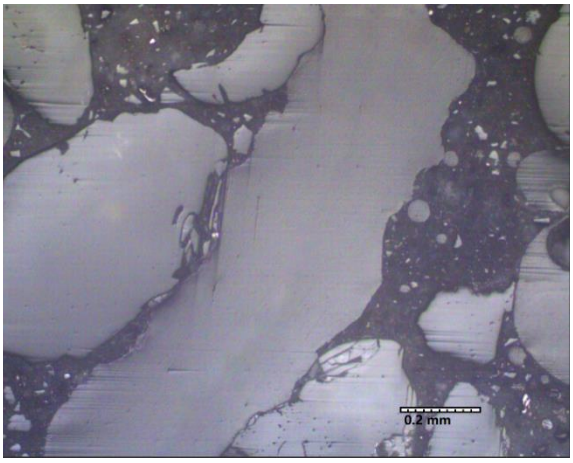

Dry-wet cycle curing

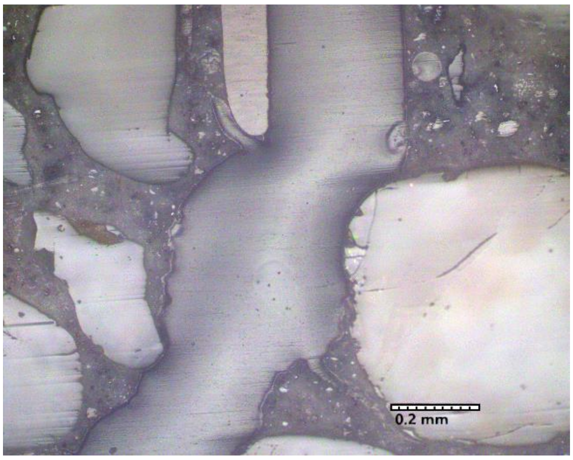

Water curing

(**a**)

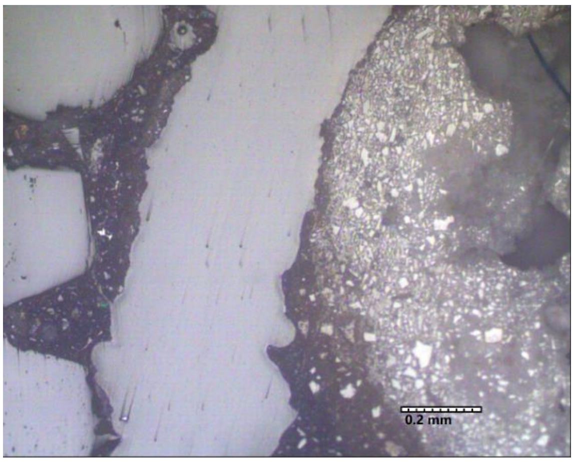

Standard curing

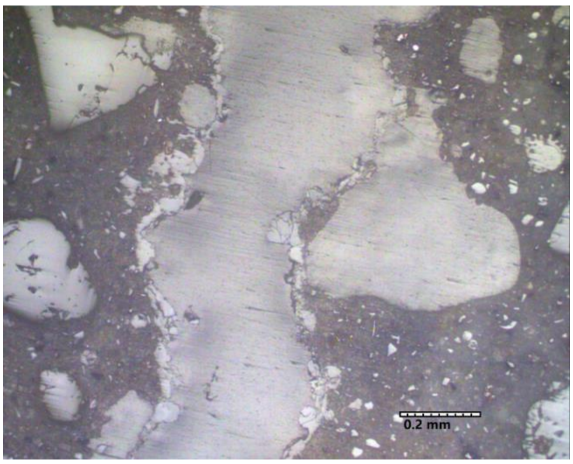

Dry-wet cycle curing

Figure 9. *Cont*.

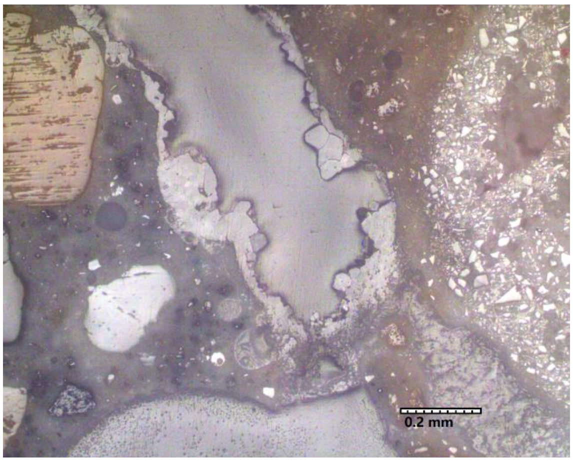

Water curing

(**b**)

Figure 9. Healing products in deep cracks under different exposure environments: (**a**) control; (**b**) with bacteria.

4. Conclusions

The self-healing cement mortar based on the artificial-functional-carrier-encapsulated bacteria was prepared. The crack self-healing effect of mortars with and without bacteria under different exposure environments (standard curing, dry–wet cycle curing, and water curing) was evaluated by the visual observation of surface and internal cracks, water permeability tests, and mechanical performance recovery. In addition, the internal healing products of cracks were observed using a metallographic microscope. The main conclusions are as follows:

- The mortar specimens based on the artificial-functional-carrier-encapsulated bacteria have a higher crack area repair ratio, and better water tightness regain and recovery ratio of flexural strength compared with the control mortars under the same exposure environment;
- The self-healing effect of mortar cracks with and without bacteria is obviously affected by exposure environments. The presence of water is necessary for crack self-healing. Higher self-healing efficiency is obtained under water curing and dry–wet cycle curing environments;
- The mortar specimens with bacteria generate more repair products in the surface and interior of cracks to greatly improve the self-repair ability of the specimens, which promotes the recovery of water tightness and mechanical performance.

Author Contributions: Investigation, methodology, writing—original draft, writing—review and editing, and supervision: M.L.; investigation, methodology, and writing—review and editing: Y.L.; investigation, methodology, and writing—review and editing: X.L.; writing—review and editing: J.D. All authors have read and agreed to the published version of the manuscript.

Funding: This research was funded by the National Natural Science Foundation of China (No. 51808483), Natural Science Foundation of Jiangsu Province (No. BK20180930), and China Postdoctoral Science Foundation (2021M692719).

Data Availability Statement: The data presented in this study are available on request from the corresponding authors.

Conflicts of Interest: The authors declare no conflict of interest.

References

1. Zhang, W.; Zheng, Q.F.; Ashour, A.; Han, B.G. Self-healing cement concrete composites for resilient infrastructures: A review. *Compos. Part B Eng.* **2020**, *189*, 107892. [CrossRef]
2. Zhang, P.; Wittmann, F.H.; Vogel, M.; Müller, H.S.; Zhao, T. Influence of freeze-thaw cycles on capillary absorption and chloride penetration into concrete. *Cem. Concr. Res.* **2017**, *100*, 60–67. [CrossRef]
3. Peng, J.X.; Hu, S.W.; Zhang, J.R.; Cai, C.S.; Li, L.-Y. Influence of cracks on chloride diffusivity in concrete: A five-phase mesoscale model approach. *Constr. Build. Mater.* **2018**, *197*, 587–596. [CrossRef]
4. Liu, H.; Huang, H.L.; Wu, X.T.; Peng, H.X.; Li, Z.H.; He, J.; Yu, Q.J. Effects of external multi-ions and wet-dry cycles in a marine environment on autogenous self-healing of cracks in cement paste. *Cem. Concr. Res.* **2019**, *120*, 198–206. [CrossRef]
5. Li, W.T.; Dong, B.Q.; Yang, Z.X.; Xu, J.; Chen, Q.; Li, H.X.; Xing, F.; Jiang, Z.W. Recent advances in intrinsic self-healing cementitious materials. *Adv. Mater.* **2018**, *30*, 1705679. [CrossRef] [PubMed]
6. Huang, H.L.; Ye, G.; Damidot, D. Effect of blast furnace slag on self-healing of microcracks in cementitious materials. *Cem. Concr. Res.* **2014**, *60*, 68–82. [CrossRef]
7. Huang, H.L.; Ye, G.; Qian, C.X.; Schlangen, E. Self-healing in cementitious materials: Materials, methods and service conditions. *Mater. Des.* **2016**, *92*, 499–511. [CrossRef]
8. Ramachandran, S.K.; Ramakrishnan, V.; Bang, S.S. Remediation of concrete using micro-organisms. *J. Am. Concr. Inst.* **2001**, *98*, 3–9.
9. Muynck, W.D.; Belie, N.D.; Verstraete, W. Microbial carbonate precipitation in construction materials: A review. *Ecol. Eng.* **2010**, *36*, 118–136. [CrossRef]
10. Wiktor, V.; Jonkers, H.M. Quantification of crack-healing in novel bacteria-based self-healing concrete. *Cem. Concr. Compos.* **2011**, *33*, 763–770. [CrossRef]
11. Jonkers, H.M.; Thijssen, A.; Muyzer, G.; Copuroglu, O.; Schlangen, E. Application of bacteria as self-healing agent for the development of sustainable concrete. *Ecol. Eng.* **2010**, *36*, 230–235. [CrossRef]
12. Wang, J.Y.; Dewanckele, J.; Cnudde, V.; Vlierberghe, S.V.; Verstraete, W.; Belie, N.D. X-ray computed tomography proof of bacterial-based self-healing in concrete. *Cem. Concr. Compos.* **2014**, *53*, 289–304. [CrossRef]
13. Jongvivatsakul, P.; Janprasit, K.; Nuaklong, P.; Pungrasmi, W.; Likitlersuang, S. Investigation of the crack healing performance in mortar using microbially induced calcium carbonate precipitation (MICP) method. *Constr. Build. Mater.* **2019**, *212*, 737–744. [CrossRef]
14. Zheng, T.W.; Su, Y.L.; Zhang, X.; Zhou, H.Y.; Qian, C.X. Effect and mechanism of encapsulation-based spores on self-healing concrete at different curing ages. *ACS Appl. Mater. Interfaces* **2020**, *12*, 52415–52432. [CrossRef]
15. Ruan, S.Q.; Qiu, J.S.; Weng, Y.W.; Yang, Y.; Yang, Y.-H.; Chu, J.; Unluer, C. The use of microbial induced carbonate precipitation in healing cracks within reactive magnesia cement-based blends. *Cem. Concr. Res.* **2019**, *115*, 176–188. [CrossRef]
16. Xu, J.; Wang, X.Z. Self-healing of concrete cracks by use of bacteria-containing low alkali cementitious material. *Constr. Build. Mater.* **2018**, *167*, 1–14. [CrossRef]
17. Su, Y.L.; Zheng, T.W.; Qian, C.X. Application potential of Bacillus megaterium encapsulated by low alkaline sulphoaluminate cement in self-healing concrete. *Constr. Build. Mater.* **2020**, *273*, 121740. [CrossRef]
18. Xu, J.; Wang, X.Z.; Zuo, J.Q.; Liu, X.Y. Self-healing of concrete cracks by ceramsite-loaded microorganisms. *Adv. Mater. Sci. Eng.* **2018**, *2018*, 5153041. [CrossRef]
19. Bundur, Z.B.; Kirisits, M.J.; Ferron, R.D. Use of pre-wetted lightweight fine expanded shale aggregates as internal nutrient reservoirs for microorganisms in bio-mineralized mortar. *Cem. Concr. Compos.* **2017**, *84*, 167–174. [CrossRef]
20. Shaheen, N.; Khushnood, R.A. Bioimmobilized limestone powder for autonomous healing of cementitious systems: A feasibility study. *Adv. Mater. Sci. Eng.* **2018**, *2018*, 7049121. [CrossRef]
21. Wang, J.Y.; Belie, N.D.; Verstraete, W. Diatomaceous earth as a protective vehicle for bacteria applied for self-healing concrete. *J. Indus. Microbiol. Biotech.* **2011**, *39*, 567–577. [CrossRef] [PubMed]
22. Wang, J.Y.; Snoeck, D.; Vlierberghe, S.V.; Verstraete, W.; Belie, N.D. Application of hydrogel encapsulated carbonate precipitating bacteria for approaching a realistic self-healing in concrete. *Constr. Build. Mater.* **2014**, *68*, 110–119. [CrossRef]
23. Wang, J.Y.; Mignon, A.; Trenson, G.; Vlierberghe, S.V.; Boon, N.; Belie, N.D. A chitosan based pH-responsive hydrogel for encapsulation of bacteria for self-sealing concrete. *Cem. Concr. Compos.* **2018**, *93*, 309–322. [CrossRef]
24. Wang, J.Y.; Soens, H.; Verstraete, W.; Belie, N.D. Self-healing concrete by use of microencapsulated bacterial spores. *Cem. Concr. Res.* **2014**, *56*, 139–152. [CrossRef]
25. Intarasoontron, J.; Pungrasmi, W.; Nuaklong, P.; Jongvivatsakul, P.; Likitlersuang, S. Comparing performances of MICP bacterial vegetative cell and microencapsulated bacterial spore methods on concrete crack healing. *Constr. Build. Mater.* **2021**, *302*, 124227. [CrossRef]
26. Zhang, J.G.; Liu, Y.Z.; Feng, T.; Zhou, M.J.; Zhao, L.; Zhou, A.J.; Li, Z. Immobilizing bacteria in expanded perlite for the crack self-healing in concrete. *Constr. Build. Mater.* **2017**, *148*, 610–617. [CrossRef]
27. Liu, C.; Xu, X.Y.; Lv, Z.Y.; Xing, L. Self-healing of concrete cracks by immobilizing microorganisms in recycled aggregate. *J. Adv. Concr. Technol.* **2020**, *18*, 168–178. [CrossRef]
28. Pungrasmi, W.; Intarasoontron, J.; Jongvivatsakul, P.; Likitlersuang, S. Evaluation of microencapsulation techniques for MICP bacterial spores applied in self-healing concrete. *Sci. Rep.* **2019**, *9*, 12484. [CrossRef]

29. Snoeck, D.; Belie, N.D. Repeated autogenous healing in strain-hardening cementitious composites by using superabsorbent polymers. *J. Mater. Civil. Eng.* **2016**, *28*, 04015086. [CrossRef]
30. Luo, M.; Qian, C.X.; Li, R.Y. Factors affecting crack repairing capacity of bacteria-based self-healing concrete. *Constr. Build. Mater.* **2015**, *87*, 1–7. [CrossRef]
31. Roig-Flores, M.; Moscato, S.; Serna, P.; Ferrara, L. Self-healing capability of concrete with crystalline admixtures in different environments. *Constr. Build. Mater.* **2015**, *86*, 1–11. [CrossRef]
32. Nosouhian, F.; Mostofinejad, D.; Hasheminejad, H. Concrete durability improvement in a sulfate environment using bacteria. *J. Mater. Civil. Eng.* **2016**, *28*, 04015064. [CrossRef]
33. Wang, J.Y.; Tittelboom, K.V.; Belie, N.D. Use of silica gel or polyurethane immobilized bacteria for self-healing concrete. *Constr. Build. Mater.* **2012**, *26*, 532–540. [CrossRef]
34. Luo, M.; Bai, J.Q.; Jing, K.; Ding, Z.Q.; Yang, D.Y.; Qian, C.X. Self-healing of early-age cracks in cement mortars with artificial functional aggregates. *Constr. Build. Mater.* **2021**, *272*, 121846. [CrossRef]